Counter–intuitive Stability in Actinide Encapsulated Metalloid Clusters with Broken Aromaticity

Meenakshi Joshi[†,§] Ayan Ghosh[#,§], Aditi Chandrasekar[‡,§] and Tapan K. Ghanty[†,§,*]

[†]Theoretical Chemistry Section, Chemistry Group, Bhabha Atomic Research Centre, Mumbai 400085, India.

[#]Laser and Plasma Technology Division, Beam Technology Development Group, Bhabha Atomic Research Centre, Mumbai 400085, India.

[‡]Fuel Chemistry Division, Indira Gandhi Centre for Atomic Research, Kalpakkam 603102, India.

[§] Homi Bhabha National Institute, Training School Complex, Anushakti Nagar, Mumbai–400094, India.

List of Tables

Table S1. Calculated Values of Inter–Ring (R_{inter}), Intra–Ring (R_{intra}) Bond Distances (in Å), Axial (R_{ax}) and Equatorial (R_{eq}) Bond distances (in Å) of Central Atom with Ring Atoms, HOMO−LUMO Energy Gap (ΔE_{gap}, in eV) of $U@Bi_{12}^{3-}$ and $La@Sb_{12}^{3-}$ Clusters as obtained by using PBE (B3LYP) Methods along with DEF and DEF2 basis sets. (B3LYP Calculated Properties are reported within parenthesis).

Table S2. Calculated Relative Energies (RE, in kcal mol^{-1}) of $M@E_{12}^{6-}$ (M = Th^{4+}, Pa^{5+}, U^{6+}, Np^{7+}; and La^{3+}, Ce^{4+}, Pr^{5+}, Nd^{6+}; E = Sb, and Bi) Clusters in C_s Symmetry with Respect to the Corresponding D_{3h} Isomer as obtained by using PBE/DEF Method.

Table S3. Calculated Values of Inter–Ring (R_{inter}), Intra–Ring (R_{intra}) Bond Distances (in Å) as well as Axial (R_{ax}) and Equatorial (R_{eq}) Bond distances (in Å) of Central Atom with Ring Atoms in $An@E_{12}^{6-}$ and $Ln@E_{12}^{6-}$ (An = Th^{4+}, Pa^{5+}, U^{6+}, Np^{7+}; Ln = La^{3+}, Ce^{4+}, Pr^{5+}, Nd^{6+}; and E = Sb and Bi) Clusters in D_{3h} Symmetry as obtained by using [a]B3LYP/DEF Method.

Table S4. Calculated Values of Binding Energy (BE, in eV), HOMO−LUMO Energy gap (ΔE_{gap}, in eV), and Dihedral Angle (DA, in Degree) of E_4^{2-} of $An@E_{12}^{6-}$ and $Ln@E_{12}^{6-}$ (An = Th^{4+}, Pa^{5+}, U^{6+}, Np^{7+}; Ln = La^{3+}, Ce^{4+}, Pr^{5+}, Nd^{6+}; and E = Sb and Bi) Clusters in D_{3h} Symmetry as obtained by using B3LYP/DEF Method.

Table S5. Optimized Bond Length (in, Å), HOMO–LUMO Gap (ΔE, in eV), Binding Energy (BE, in eV) and Dihedral Angle of Sb_4^{2-} Ring (DA, in degree) of $Th@Sb_{12}^{2-}$, Calculated using AVDZ (without f Function), AVTZ (with f Function) and of $La@Sb_{12}^{3-}$ Calculated using def–TZVP (without f Function), def–TZVPP (with f Function) and for Th–O, Bond Length (in, Å), HOMO–LUMO Gap (ΔE, in eV), Binding Energy (BE, in eV) Calculated using AVDZ (without f Function), AVTZ (with f Function) Basis Sets. For Sb and O, def–TZVPP basis set is used.

Table S6. Calculated VDD Charge on the in Plane Atoms (q_{eq}), Out of Plane Atoms (q_{ax}) Overall VDD charge on Ring (q_{ring}) and f Atomic Population (f_M) of Central atoms of the $An@E_{12}^{6-}$ and $Ln@E_{12}^{6-}$ (An = Th^{4+}, Pa^{5+}, U^{6+}, Np^{7+}; Ln = La^{3+}, Ce^{4+}, Pr^{5+}, Nd^{6+}; and E = Sb and Bi) Clusters using Voronoi Deformation Density (VDD) and Natural Population

Analysis (NPA) as obtained by using PBE/TZ2P and PBE/DEF (B3LYP/ DEF) Methods, respectively.(B3LYP calculated Atomic Population is given in the parenthesis)

Table S7. Calculated Values of Bond Critical Point Electron Density (ρ in e a_0^{-3}), Laplacian of Electron Density ($\nabla^2\rho$ in e a_0^{-5}), Local Electron Energy Density (E_d in au), and Ratio of Local Electron Kinetic Energy Density and Electron Density ($G(r)/\rho$ in au) of $An@Sb_{12}^{6-}$ (An = Th^{4+}, Pa^{5+}, U^{6+}, Np^{7+}) Clusters as obtained by using ^{a}PBE Method along with ^{b}Small Core ECP Employed with EDF.

Table S8. Calculated Values of Bond Critical Point Electron Density (ρ in e a_0^{-3}), Laplacian of Electron Density ($\nabla^2\rho$ in e a_0^{-5}), Local Electron Energy Density (E_d in au), and Ratio of Local Electron Kinetic Energy Density and Electron Density ($G(r)/\rho$ in au) of $Ln@Sb_{12}^{6-}$ (Ln = La^{3+}, Ce^{4+}, Pr^{5+}, Nd^{6+}) Clusters as obtained by using ^{a}PBE Method along with ^{b}Small Core ECP Employed with EDF.

Table S9. Calculated Values of Bond Critical Point Electron Density (ρ in e a_0^{-3}), Laplacian of Electron Density ($\nabla^2\rho$ in e a_0^{-5}), Local Electron Energy Density (E_d in au), and Ratio of Local Electron Kinetic Energy Density and Electron Density ($G(r)/\rho$ in au) of $An@Bi_{12}^{6-}$ (An = Th^{4+}, Pa^{5+}, U^{6+}, Np^{7+}) Clusters as obtained by using ^{a}PBE Method along with ^{b}Small Core ECP Employed with EDF.

Table S10. Calculated Values of Bond Critical Point Electron Density (ρ in e a_0^{-3}), Laplacian of Electron Density ($\nabla^2\rho$ in e a_0^{-5}), Local Electron Energy Density (E_d in au), and Ratio of Local Electron Kinetic Energy Density and Electron Density ($G(r)/\rho$ in au) of $Ln@Bi_{12}^{6-}$ (Ln = La^{3+}, Ce^{4+}, Pr^{5+}, Nd^{6+}) Clusters as obtained by using ^{a}PBE Method along with ^{b}Small Core ECP Employed with EDF.

Table S11. Calculated Vibrational Frequencies (in cm^{-1}) as Obtained by using PBE/DEF Method for $Ln@Sb_{12}^{6-}$ and $Ln@Bi_{12}^{6-}$ Clusters. (Absorption Intensities in km mol^{-1} and Symmetry are Provided in Parenthesis.)

Table S12. Calculated Vibrational Frequencies (in cm^{-1}) as Obtained by using PBE/DEF Method for $An@Sb_{12}^{6-}$ and $An@Bi_{12}^{6-}$ Clusters. (Intensities in km mol^{-1} and Symmetry are Provided in Parenthesis.)

List of Figures

Figure S1. Molecular orbital energy level diagram of $Ln@Sb_{12}^{6-}$ (Ln = La^{3+}, Ce^{4+}, Pr^{5+}, Nd^{6+}) clusters in D_{3h} symmetry as obtained by using PBE/DEF method. (Where blue lines represents mixed MOs having orbital contribution from central metal ion and ring atoms, red lines stands for the MOs corresponding to the pure orbital of ring atoms only and green lines stands for small mixed MOs having small contribution of central ion orbitals Here, the s block refers to the valence s−orbitals of Sb atoms)

Figure S2. Molecular orbital pictures of $Th@Sb_{12}^{2-}$ cluster in D_{3h} symmetry as obtained by using PBE/DEF method. (Where M stands for mixed MOs having orbital contribution from central metal atom and ring atoms, P stands for MOs corresponds to pure orbital of ring atoms alone)

Figure S3. Molecular orbital pictures of $La@Sb_{12}^{3-}$ cluster in D_{3h} symmetry as obtained by using PBE/DEF method. (Where M stands for mixed MOs having orbital contribution from central metal ion and ring atoms, P stands for MOs corresponds to pure orbital of ring atoms only and S−M stands for those MOs which are formed by the overlapping of atomic orbital of ring atoms and have very small overlapping with the atomic orbital of central atom)

Figure S4. Molecular orbital pictures of $U@Sb_{12}$ cluster in D_{3h} symmetry as obtained by using PBE/DEF method. (Where M stands for mixed MOs having orbital contribution from central metal atom and ring atoms, P stands for MOs corresponds to pure orbital of ring atoms alone.)

Figure S5. Molecular orbital pictures of $Nd@Sb_{12}$ cluster in D_{3h} symmetry as obtained by using PBE/DEF method. (Where M stands for mixed MOs having orbital contribution from central metal ion and ring atoms, P stands for MOs corresponds to pure orbital of ring atoms

only and S−M stands for those MOs which are formed by the overlapping of atomic orbital of ring atoms and have very small overlapping with the atomic orbital of central atom)

Figure S6. Density of states plots of $Ln@Sb_{12}^{6-}$ ($Ln = La^{3+}$, Ce^{4+}, Pr^{5+}, Nd^{6+}) clusters in D_{3h} symmetry as obtained by using PBE/DEF method. (Arrows are showing peak corresponding to HOMO).

Figure S7. Density of states plots of (a) $Ln@Bi_{12}^{6-}$ ($Ln = La^{3+}$, Ce^{4+}, Pr^{5+}, Nd^{6+}) clusters and (b) $An@Bi_{12}^{6-}$ ($An = Th^{4+}$, Pa^{5+}, U^{6+}, Np^{7+}) clusters in D_{3h} symmetry as obtained by using PBE/DEF method. (Arrows are showing peak corresponding to HOMO).

Figure S8. Laplacian of electron density plots (a1 & a2) and Electron density plots (b1 & b2) of $Ln@Sb_{12}^{6-}$ and $An@Sb_{12}^{6-}$ clusters, respectively, in D_{3h} symmetry as obtained by using PBE/DEF method employed with EDF. (Blue dots are Bond critical point (BCP) and orange dots are ring critical point (RCP))

Figure S9. Laplacian of electron density plots (a1 & a2) and Electron density plots (b1 & b2) of $Ln@Bi_{12}^{6-}$ and $An@Bi_{12}^{6-}$ clusters, respectively, in D_{3h} symmetry as obtained by using PBE/DEF method employed with EDF. (Blue dots are bond BCP and orange dots are ring critical point (RCP))

Figure S10. Harmonic frequency plots of (a) $Ln@Sb_{12}^{6-}$ and (b) $An@Sb_{12}^{6-}$ clusters, respectively, in D_{3h} symmetry as obtained by using PBE/DEF method.

Figure S11. Harmonic frequency plots of (a) $Ln@Bi_{12}^{6-}$ and (b) $An@Bi_{12}^{6-}$ clusters, respectively, in D_{3h} symmetry as obtained by using PBE/DEF method.

Figure S12. Scalar relativistic (left panel) and spin orbit splitting (right panel) diagram of the valence molecular orbital energy levels of $Nd@Bi_{12}$ system.

Figure S13. Scalar relativistic (left panel) and spin orbit splitting (right panel) diagram of the valence molecular orbital energy levels of $Nd@Sb_{12}$ system.

Figure S14. Scalar relativistic (left panel) and spin orbit splitting (right panel) diagram of the valence molecular orbital energy levels of U@Sb_{12} system.

Table S1. Calculated Values of Inter–Ring (R_{inter}), Intra–Ring (R_{intra}) Bond Distances (in Å), Axial (R_{ax}) and Equatorial (R_{eq}) Bond distances (in Å) of Central Atom with Ring Atoms, HOMO−LUMO Energy Gap (ΔE_{gap}, in eV) of $U@Bi_{12}^{3-}$ and $La@Sb_{12}^{3-}$ Clusters as obtained by using PBE (B3LYP) Methods along with DEF and DEF2 basis sets. (B3LYP Calculated Properties are reported within parenthesis)

Systems	Method	R_{eq}	R_{ax}	R_{intra}	R_{inter}	ΔE_{gap}
$U@Bi_{12}^{3-}$	Expt	3.463 − 3.545	3.119 − 3.167	3.051 − 3.109	3.018 − 3.046	…
	[a]DEF	3.567 (3.664)	3.133 (3.236)	3.100 (3.073)	3.006 (3.085)	0.20 (0.79)
	[b]DEF2	3.592 (3.693)	3.158 (3.261)	3.107 (3.076)	3.020 (3.105)	0.15 (0.79)
$La@Sb_{12}^{3-}$	Expt	3.434 − 3.474	3.239 − 3.263	2.809 − 2.826	3.018 − 3.052	…
	[a]DEF	3.542 (3.588)	3.334 (3.384)	2.865 (2.865)	3.136 (3.168)	1.17 (1.96)
	[c]DEF2	3.529 (3.583)	3.310 (3.365)	2.870 (2.872)	3.121 (3.150)	1.05 (1.84)

[a]For all atoms def−TZVPP basis set is used.
[b]For U def−TZVPP basis set is used, while for Bi, def2−TZVPP basis set has been used.
[c]For La, Stuttgart basis set is used, while for Sb, def2−TZVPP basis set has been used.

Table S2. Calculated Relative Energy (RE, in kcal mol^{-1}) of $M@E_{12}^{6-}$ (M = Th^{4+}, Pa^{5+}, U^{6+}, Np^{7+}; and La^{3+}, Ce^{4+}, Pr^{5+}, Nd^{6+}; E = Sb, and Bi) Clusters in C_s Symmetry with Respect to the Corresponding D_{3h} Isomer as obtained by using PBE/DEF Method.

Systems	RE	
	D_{3h}	C_s
$Th@Bi_{12}^{2-}$	0.00	14.32
$Pa@Bi_{12}^{-}$	0.00	15.85
$U@Bi_{12}$	0.00	12.26
$Np@Bi_{12}^{+}$	0.00	8.49
$Th@Sb_{12}^{2-}$	0.00	14.57
$Pa@Sb_{12}^{-}$	0.00	16.12
$U@Sb_{12}$	0.00	12.48
$Np@Sb_{12}^{+}$	0.00	8.15
$La@Bi_{12}^{3-}$	0.00	7.62
$Ce@Bi_{12}^{2-}$	0.00	10.56
$Pr@Bi_{12}^{-}$	0.00	7.54
$Nd@Bi_{12}$	0.00	...[a]
$La@Sb_{12}^{3-}$	0.00	6.10
$Ce@Sb_{12}^{2-}$	0.00	11.88
$Pr@Sb_{12}^{-}$	0.00	9.06
$Nd@Sb_{12}$	0.00	...[a]

[a]Could not be calculated

Table S3. Calculated Values of Inter–Ring (R_{inter}), Intra–Ring (R_{intra}) Bond Distances (in Å) as well as Axial (R_{ax}) and Equatorial (R_{eq}) Bond distances (in Å) of Central Atom with Ring Atoms in An@E_{12}^{6-} and Ln@E_{12}^{6-} (An = Th^{4+}, Pa^{5+}, U^{6+}, Np^{7+}; Ln = La^{3+}, Ce^{4+}, Pr^{5+}, Nd^{6+}; and E = Sb and Bi) Clusters in D_{3h} Symmetry as obtained by using [a]B3LYP/DEF Method.

Systems	R_{eq}	R_{ax}	R_{intra}	R_{inter}
Th@Bi_{12}^{2-}	3.653	3.326	3.031	3.185
Pa@Bi_{12}^{-}	3.542	3.190	3.044	3.101
U@Bi_{12}	3.488	3.127	3.059	3.060
Np@Bi_{12}^{+}	3.467	3.112	3.074	3.049
Th@Sb_{12}^{2-}	3.519	3.268	2.865	3.092
Pa@Sb_{12}^{-}	3.412	3.125	2.879	2.987
U@Sb_{12}	3.345	3.049	2.899	2.922
Np@Sb_{12}^{+}	3.320	3.028	2.912	2.896
La@Bi_{12}^{3-}	3.730	3.446	3.032	3.245
Ce@Bi_{12}^{2-}	3.603	3.245	3.038	3.146
[a]Pr@Bi_{12}^{-}	3.543	3.164	3.060	3.092
[a]Nd@Bi_{12}	3.451	3.157	3.078	3.054
Ce@Sb_{12}^{2-}	3.473	3.195	2.867	3.043
[a]Pr@Sb_{12}^{-}	3.399	3.096	2.895	2.961
Nd@Sb_{12}	3.374	3.064	2.911	2.932

[a]B3LYP optimized structures of Pr@Bi_{12}^{-}, Pr@Sb_{12}^{-} and Nd@Bi_{12} are associated with the imaginary frequency values.

Table S4. Calculated Values of Binding Energy (BE, in eV), HOMO−LUMO Energy gap (ΔE_{gap}, in eV), and Dihedral Angle (DA, in Degree) of E_4^{2-} of An@E_{12}^{6-} and Ln@E_{12}^{6-} (An = Th^{4+}, Pa^{5+}, U^{6+}, Np^{7+}; Ln = La^{3+}, Ce^{4+}, Pr^{5+}, Nd^{6+}; and E = Sb and Bi) Clusters in D_{3h} Symmetry as obtained by using B3LYP/DEF Method.

Systems	BE	ΔE_{gap}	DA	Systems	BE	ΔE_{gap}	DA
Th@Bi_{12}^{2-}	−79.97	2.04	19.0	**Th@Sb_{12}^{2-}**	−79.85	2.42	15.0
Pa@Bi_{12}^{-}	−127.73	2.15	24.0	**Pa@Sb_{12}^{-}**	−127.54	2.44	20.1
U@Bi_{12}	−191.54	2.21	26.6	**U@Sb_{12}**	−191.08	2.28	23.1
Np@Bi_{12}^{+}	−273.82	1.97	27.6	**Np@Sb_{12}^{+}**	−272.88	2.14	24.2
U@Bi_{12}^{3-}	−37.23	0.79		...	...	...	...
La@Bi_{12}^{3-}	−45.12	1.81	14.8	**La@Sb_{12}^{3-}**	−44.89	1.96	11.1
Ce@Bi_{12}^{2-}	−86.65	1.95	22.0	**Ce@Sb_{12}^{2-}**	−86.47	2.10	17.4
Pr@Bi_{12}^{-}	−146.73	1.71	25.3	**Pr@Sb_{12}^{-}**	−146.28	1.75	21.4
Nd@Bi_{12}	−229.49	1.25	26.3	**Nd@Sb_{12}**	−228.66	1.76	22.8

Table S5. Optimized Bond Length (in, Å), HOMO–LUMO Gap (ΔE, in eV), Binding Energy (BE, in eV) and Dihedral Angle of Sb_4^{2-} Ring (DA, in degree) of Th@Sb_{12}^{2-}, Calculated using AVDZ (without f Function), AVTZ (with f Function) and of La@Sb_{12}^{3-} Calculated using def–TZVP (without f Function), def–TZVPP (with f Function) and for Th–O, Bond Length (in, Å), HOMO–LUMO Gap (ΔE, in eV), Binding Energy (BE, in eV) Calculated using AVDZ (without f Function), AVTZ (with f Function) Basis Sets. For Sb and O, def–TZVPP basis set is used.

Systems	Basis set for Th/La	R_{ax}/Th–O	R_{eq}	R_{inter}	R_{intra}	BE	ΔE	DA
La@Sb_{12}^{3-}	def–TZVP-without f	3.342	3.547	3.142	2.866	–46.54	1.16	12.6
La@Sb_{12}^{3-}	def–TZVPP-with f	3.334	3.542	3.136	2.865	–46.64	1.17	12.9
Th@Sb_{12}^{2-}	AVDZ- without f	3.276	3.504	3.108	2.866	–80.90	1.59	15.1
Th@Sb_{12}^{2-}	AVTZ-with f	3.228	3.464	3.066	2.870	–81.57	1.53	16.7
Th@Sb_{12}^{2-}	def-TZVPP-with f	3.218	3.456	3.053	2.872	−82.36	1.50	17.0
Th–O	AVDZ-without f	1.984	...	...	...	–7.87	1.00	...
Th–O	AVTZ-with f	1.840	...	...	...	–9.64	1.19	...
Th–O[96]	CASSCF-without f	2.025	...	...	...	–7.02	...	...
Th–O[96]	CASSCF-with f	1.882	...	...	...	–8.92	...	...

Table S6. Calculated VDD Charge on the in Plane Atoms (q_{eq}), Out of Plane Atoms (q_{ax}) Overall VDD charge on Ring (q_{ring}) and f Atomic Population (f_M) of Central atoms of the An@E_{12}^{6-} and Ln@E_{12}^{6-}(An = Th^{4+}, Pa^{5+}, U^{6+}, Np^{7+}; Ln = La^{3+}, Ce^{4+}, Pr^{5+}, Nd^{6+}; and E = Sb and Bi) Clusters using Voronoi Deformation Density (VDD) and Natural Population Analysis (NPA) as obtained by using PBE/TZ2P and PBE/DEF (B3LYP/ DEF) Methods, respectively.(B3LYP calculated Atomic Population is given in the parenthesis)

Systems	q_{eq}	q_{ax}	q_{ring}	q_M	f_M
Th@Bi_{12}^{2-}	−0.12	−0.21	−2.01	0.01	3.48 (2.79)
Pa@Bi_{12}^{-}	−0.05	−0.12	−1.05	0.05	3.50(2.30)
U@Bi_{12}	0.03	−0.03	0.02	−0.02	4.07 (3.81)
Np@Bi_{12}^{+}	0.11	0.07	1.07	−0.07	5.04 (4.82)
Th@Sb_{12}^{2-}	−0.15	−0.22	−2.03	0.03	3.30(3.23)
Pa@Sb_{12}^{-}	−0.04	−0.13	−1.07	0.07	3.69 (2.82)
U@Sb_{12}	0.04	−0.03	0.01	−0.01	4.29(3.16)
Np@Sb_{12}^{+}	0.12	0.06	1.06	−0.06	5.23 (4.01)
La@Bi_{12}^{3-}	−0.19	−0.30	−2.95	−0.05	0.004(0.003)
Ce@Bi_{12}^{2-}	−0.12	−0.19	−1.85	−0.15	1.23 (0.97)
Pr@Bi_{12}^{-}	−0.05	−0.11	−0.95	−0.04	2.40(2.22)
Nd@Bi_{12}	0.03	−0.02	0.06	−0.06	3.54 (3.41)
La@Sb_{12}^{3-}	−0.19	−0.31	−2.97	−0.03	0.003(0.002)
Ce@Sb_{12}^{2-}	−0.11	−0.21	−1.87	−0.12	1.19 (0.94)
Pr@Sb_{12}^{-}	−0.04	−0.12	−0.99	−0.02	2.40 (2.20)
Nd@Sb_{12}	0.04	−0.03	0.05	−0.05	3.56(3.39)

Table S7. Calculated Values of Bond Critical Point Electron Density (ρ in e a_0^{-3}), Laplacian of Electron Density ($\nabla^2\rho$ in e a_0^{-5}), Local Electron Energy Density (E_d in au), and Ratio of Local Electron Kinetic Energy Density and Electron Density ($G(r)/\rho$ in au) of $An@Sb_{12}^{6-}$ (An = Th^{4+}, Pa^{5+}, U^{6+}, Np^{7+}) Clusters as obtained by using [a]PBE Method along with [b]Small Core ECP Employed with EDF.

Systems	Bond	ρ	$\nabla^2\rho$	G(r)[c]	V(r)[d]	E_d(r)	G(r)/ρ	Type[e]
$Th@Sb_{12}^{2-}$	$R_{ax(Th-Sb)}$	0.038	0.026	0.015	−0.023	−0.008	0.378	C, D
	$R_{eq(Th-Sb)}$	0.024	0.033	0.011	−0.014	−0.003	0.461	C, D
	$R_{intra(Sb-Sb)}$	0.052	0.008	0.016	−0.029	−0.014	0.299	C, D
	$R_{inter(Sb-Sb)}$	0.041	0.013	0.011	−0.019	−0.008	0.270	C,D
$Pa@Sb_{12}^{-}$	$R_{ax(Pa-Sb)}$	0.048	0.021	0.018	−0.031	−0.013	0.376	C,D
	$R_{eq(Pa-Sb)}$	0.030	0.032	0.013	−0.018	−0.005	0.435	C,D
	$R_{intra(Sb-Sb)}$	0.050	0.010	0.015	−0.028	−0.013	0.304	C,D
	$R_{inter(Sb-Sb)}$	0.047	0.010	0.013	−0.024	−0.011	0.282	C,D
$U@Sb_{12}$	$R_{ax(U-Sb)}$	0.052	0.019	0.020	−0.035	−0.015	0.375	C,D
	$R_{eq(U-Sb)}$	0.032	0.032	0.014	−0.019	−0.006	0.428	C,D
	$R_{intra(Sb-Sb)}$	0.050	0.011	0.015	−0.028	−0.013	0.305	C,D
	$R_{inter(Sb-Sb)}$	0.050	0.009	0.014	−0.027	−0.012	0.290	C,D
$Np@Sb_{12}^{+}$	$R_{ax(Np-Sb)}$	0.053	0.019	0.020	−0.035	−0.015	0.380	C,D
	$R_{eq(Np-Sb)}$	0.032	0.033	0.014	−0.019	−0.006	0.432	C,D
	$R_{intra(Sb-Sb)}$	0.049	0.011	0.015	−0.027	−0.012	0.304	C,D
	$R_{inter(Sb-Sb)}$	0.051	0.008	0.015	−0.027	−0.013	0.287	C,D

[a]For Sb, def2−TZVPP basis set is used while for all An, def−TZVPP basis set is used. [b]Small Core ECP has been used for all heavy atoms viz., An (ECP 60) and Sb (ECP 28). [c]G(r) represents the local electron kinetic energy density. [d]V(r) signifies the local electron potential energy density. [e]"Type" is an indication of type of weak covalent bonding exists in between the corresponding pair of bonding atoms.

Table S8. Calculated Values of Bond Critical Point Electron Density (ρ in e a_0^{-3}), Laplacian of Electron Density ($\nabla^2\rho$ in e a_0^{-5}), Local Electron Energy Density (E_d in au), and Ratio of Local Electron Kinetic Energy Density and Electron Density ($G(r)/\rho$ in au) of $Ln@Sb_{12}^{6-}$ (Ln = La^{3+}, Ce^{4+}, Pr^{5+}, Nd^{6+}) Clusters as obtained by using [a]PBE Method along with [b]Small Core ECP Employed with EDF.

Systems	Bond	ρ	$\nabla^2\rho$	G(r)[c]	V(r)[d]	$E_d(r)$	G(r)/ρ	Type[e]
$La@Sb_{12}^{3-}$	$R_{ax(La-Sb)}$	0.028	0.032	0.011	−0.015	−0.003	0.409	C, D
	$R_{eq(La-Sb)}$	0.018	0.032	0.009	−0.001	−0.001	0.495	C, D
	$R_{intra(Sb-Sb)}$	0.053	0.007	0.016	−0.029	−0.014	0.297	C, D
	$R_{inter(Sb-Sb)}$	0.038	0.014	0.010	−0.016	−0.006	0.263	C,D
$Ce@Sb_{12}^{2-}$	$R_{ax(Ce-Sb)}$	0.038	0.032	0.015	−0.022	−0.007	0.394	C,D
	$R_{eq(Ce-Sb)}$	0.023	0.037	0.011	−0.013	−0.002	0.482	C,D
	$R_{intra(Sb-Sb)}$	0.052	0.008	0.015	−0.029	−0.013	0.298	C,D
	$R_{inter(Sb-Sb)}$	0.044	0.012	0.012	−0.021	−0.009	0.273	C,D
$Pr@Sb_{12}^{-}$	$R_{ax(Pr-Sb)}$	0.042	0.034	0.017	−0.025	−0.008	0.404	C,D
	$R_{eq(Pr-Sb)}$	0.025	0.039	0.012	−0.015	−0.003	0.482	C,D
	$R_{intra(Sb-Sb)}$	0.050	0.010	0.015	−0.028	−0.013	0.297	C,D
	$R_{inter(Sb-Sb)}$	0.048	0.009	0.013	−0.025	−0.011	0.280	C,D
$Nd@Sb_{12}$	$R_{ax(Nd-Sb)}$	0.043	0.035	0.018	−0.026	−0.009	0.411	C,D
	$R_{eq(Nd-Sb)}$	0.026	0.040	0.013	−0.015	−0.003	0.490	C,D
	$R_{intra(Sb-Sb)}$	0.050	0.098	0.015	−0.027	−0.012	0.298	C,D
	$R_{inter(Sb-Sb)}$	0.049	0.078	0.014	−0.026	−0.012	0.281	C,D

[a]For La, Stuttgart basis set is used while for all other Ln def−TZVPP basis set is used and for Sb, def2−TZVPP basis set is used. [b]Small Core ECP has been used for all heavy atoms viz., Ln (ECP 28) and Sb (ECP 28). [c]G(r) represents the local electron kinetic energy density. [d]V(r) signifies the local electron potential energy density. [e]"Type" is an indication of type of weak covalent bonding exists in between the corresponding pair of bonding atoms.

Table S9. Calculated Values of Bond Critical Point Electron Density (ρ in e a_0^{-3}), Laplacian of Electron Density ($\nabla^2\rho$ in e a_0^{-5}), Local Electron Energy Density (E_d in au), and Ratio of Local Electron Kinetic Energy Density and Electron Density ($G(r)/\rho$ in au) of $An@Bi_{12}^{6-}$ ($An = Th^{4+}$, Pa^{5+}, U^{6+}, Np^{7+}) Clusters as obtained by using [a]PBE Method along with [b]Small Core ECP Employed with EDF.

Systems	Bond	ρ	$\nabla^2\rho$	G(r)[c]	V(r)[d]	E_d(r)	G(r)/ρ	Type[e]
$Th@Bi_{12}^{2-}$	$R_{ax(Th-Bi)}$	0.036	0.026	0.014	−0.021	−0.071	0.380	C, D
	$R_{eq(Th-Bi)}$	0.021	0.027	0.009	−0.011	−0.002	0.429	C, D
	$R_{intra(Bi-Bi)}$	0.043	0.029	0.016	−0.024	−0.008	0.359	C, D
	$R_{inter(Bi-Bi)}$	0.037	0.025	0.012	−0.018	−0.006	0.324	C,D
$Pa@Bi_{12}^{-}$	$R_{ax(Pa-Bi)}$	0.044	0.025	0.017	−0.027	−0.011	0.383	C,D
	$R_{eq(Pa-Bi)}$	0.025	0.027	0.010	−0.014	−0.004	0.406	C,D
	$R_{intra(Bi-Bi)}$	0.043	0.029	0.015	−0.023	−0.008	0.362	C,D
	$R_{inter(Bi-Bi)}$	0.041	0.027	0.014	−0.022	−0.007	0.342	C,D
$U@Bi_{12}$	$R_{ax(U-Bi)}$	0.047	0.025	0.018	−0.030	−0.012	0.385	C,D
	$R_{eq(U-Bi)}$	0.027	0.027	0.011	−0.015	−0.004	0.400	C,D
	$R_{intra(Bi-Bi)}$	0.042	0.029	0.015	−0.023	−0.008	0.362	C,D
	$R_{inter(Bi-Bi)}$	0.043	0.027	0.015	−0.023	−0.008	0.347	C,D
$Np@Bi_{12}^{+}$	$R_{ax(Np-Bi)}$	0.047	0.026	0.018	−0.030	−0.012	0.391	C,D
	$R_{eq(Np-Bi)}$	0.026	0.028	0.011	−0.014	−0.004	0.406	C,D
	$R_{intra(Bi-Bi)}$	0.042	0.029	0.015	−0.023	−0.008	0.358	C,D
	$R_{inter(Bi-Bi)}$	0.043	0.026	0.015	−0.023	−0.008	0.346	C,D

[a]For Bi, def2−TZVPP basis set is used while for all An, def−TZVPP basis set is used. [b]Small Core ECP has been used for all heavy atoms viz., An (ECP 60) and Bi (ECP 60). [c]G(r) represents the local electron kinetic energy density. [d]V(r) signifies the local electron potential energy density. [e]"Type" is an indication of type of weak covalent bonding exists in between the corresponding pair of bonding atoms.

Table S10. Calculated Values of Bond Critical Point Electron Density (ρ in e a_0^{-3}), Laplacian of Electron Density ($\nabla^2\rho$ in e a_0^{-5}), Local Electron Energy Density (E_d in au), and Ratio of Local Electron Kinetic Energy Density and Electron Density ($G(r)/\rho$ in au) of Ln@Bi_{12}^{6-} (Ln = La^{3+}, Ce^{4+}, Pr^{5+}, Nd^{6+}) Clusters as obtained by using [a]PBE Method along with [b]Small Core ECP Employed with EDF.

Systems	Bond	ρ	$\nabla^2\rho$	G(r)[c]	V(r)[d]	E_d(r)	G(r)/ρ	Type[e]
La@Bi_{12}^{3-}	$R_{ax(La-Bi)}$	0.027	0.030	0.011	−0.014	−0.003	0.396	C,D
	$R_{eq(La-Bi)}$	0.016	0.026	0.007	−0.008	−0.001	0.468	C, D
	$R_{intra(Bi-Bi)}$	0.044	0.029	0.016	−0.024	−0.008	0.355	C, D
	$R_{inter(Bi-Bi)}$	0.034	0.024	0.011	−0.015	−0.005	0.311	C,D
Ce@Bi_{12}^{2-}	$R_{ax(Ce-Bi)}$	0.035	0.034	0.014	−0.020	−0.006	0.403	C,D
	$R_{eq(Ce-Bi)}$	0.020	0.030	0.009	−0.010	−0.013	0.452	C,D
	$R_{intra(Bi-Bi)}$	0.043	0.029	0.015	−0.023	−0.008	0.356	C,D
	$R_{inter(Bi-Bi)}$	0.039	0.026	0.013	−0.020	−0.007	0.330	C,D
Pr@Bi_{12}^{-}	$R_{ax(Pr-Bi)}$	0.037	0.035	0.015	−0.022	−0.007	0.410	C,D
	$R_{eq(Pr-Bi)}$	0.021	0.031	0.010	−0.011	−0.002	0.452	C,D
	$R_{intra(Bi-Bi)}$	0.042	0.028	0.015	−0.023	−0.008	0.355	C,D
	$R_{inter(Bi-Bi)}$	0.041	0.026	0.014	−0.022	−0.008	0.339	C,D
Nd@Bi_{12}	$R_{ax(Nd-Bi)}$	0.038	0.036	0.016	−0.022	−0.007	0.414	C,D
	$R_{eq(Nd-Bi)}$	0.021	0.032	0.010	−0.011	−0.002	0.458	C,D
	$R_{intra(Bi-Bi)}$	0.042	0.028	0.015	−0.023	−0.008	0.352	C,D
	$R_{inter(Bi-Bi)}$	0.042	0.026	0.014	−0.022	−0.008	0.340	C,D

[a]For La, Stuttgart basis set is used while for all other Ln def−TZVPP basis set is used and for Bi, def2−TZVPP basis set is used. [b]Small Core ECP has been used for all heavy atoms viz., Ln (ECP 28) and Bi (ECP 60). [c]G(r) represents the local electron kinetic energy density. [d]V(r) signifies the local electron potential energy density. [e]"Type" is an indication of type of weak covalent bonding exists in between the corresponding pair of bonding atoms.

Table S11. Calculated Vibrational Frequencies (in cm^{-1}) as obtained by using PBE/DEF Method for Ln@Sb_{12}^{6-} and Ln@Bi_{12}^{6-} Clusters (Absorption Intensities in km mol^{-1} and Symmetry are Provided in Parenthesis).

La@Sb_{12}^{3-}	Ce@Sb_{12}^{2-}	Pr@Sb_{12}^{-}	Nd@Sb_{12}	La@Bi_{12}^{3-}	Ce@Bi_{12}^{2-}	Pr@Bi_{12}^{-}	Nd@Bi_{12}
16.64 (a_2'') (0.762)	17.81 (a_2'') (0.394)	28.28 (a_2'') (0.308)	30.07 (e'') (0.000)	7.72 (a_2'') (0.728)	24.71 (a_2'') (0.468)	27.81 (e'') (0.000)	21.21 (e'') (0.000)
29.62 (e'') (0.000)	34.78 (e'') (0.000)	35.02 (e'') (0.000)	37.05 (a_2'') (0.226)	20.73 (e'') (0.000)	27.73 (e'') (0.000)	34.88 (a_2'') (0.348)	30.7 (e') (0.047)
38.07 (e') (0.309)	46.72 (e') (0.097)	48.06 (e') (0.061)	45.59 (e') (0.066)	27.68 (e') (0.099)	35.36 (e') (0.020)	35.14 (e') (0.018)	32.37 (a_1'') (0.000)
44.44 (a_1'') (0.000)	49.19 (a_1') (0.000)	50.6 (a_1'') (0.000)	50.59 (a_1'') (0.000)	32.47 (a_1'') (0.000)	36.75 (a_1'') (0.000)	35.90 (a_1'') (0.000)	38.68 (a_2'') (0.281)
54.43 (a_1') (0.000)	49.89 (a_1'') (0.000)	58.54 (a_1') (0.000)	61.57 (a_2') (0.000)	34.93 (a_1') (0.000)	38.48 (a_1') (0.000)	41.46 (a_2') (0.000)	39.02 (a_2') (0.000)
67.51 (e') (0.448)	70.68 (a_2') (0.000)	64.23 (a_2') (0.000)	65.89 (a_1') (0.000)	46.98 (e') (0.262)	45.13 (a_2') (0.000)	47.77 (a_1') (0.000)	45.32 (e') (0.012)
76.46 (e'') (0.000)	71.14 (e') (0.411)	71.32 (e') (0.242)	69.61 (e') (0.126)	53.05 (a_2') (0.000)	49.45 (e') (0.112)	48.69 (e') (0.047)	52.57 (a_1') (0.000)
79.84 (a_2') (0.000)	88.75 (e'') (0.000)	92.94 (e'') (0.000)	91.87 (e'') (0.000)	56.28 (e'') (0.000)	64.7 (e'') (0.000)	64.45 (e'') (0.000)	61.61 (e'') (0.000)
85.85 (e') (1.938)	96.14 (e') (1.099)	101.92 (e') (0.251)	104.1 (a_1') (0.000)	65.42 (e') (0.785)	69.23 (e') (0.107)	72.07 (e') (0.003)	73.59 (e') (0.042)
93.94 (a_1') (0.000)	102.14 (a_1') (0.000)	104.15 (a_1') (0.000)	104.45 (e') (0.036)	68.45 (a_1') (0.000)	76.33 (a_1') (0.000)	78.29 (a_1') (0.000)	79.12 (a_1') (0.000)
99.65 (a_1') (0.000)	118.29 (e') (0.459)	128.51 (e') (0.623)	127.93 (e') (0.872)	79.93 (e') (0.764)	95.37 (a_1') (0.000)	98.04 (e'') (0.000)	94.84 (a_1'') (0.000)
101.32 (e') (0.003)	120.62 (a_1') (0.000)	131.92 (a_1') (0.000)	132.45 (a_2'') (0.070)	82.19 (a_1') (0.000)	97.27 (e') (0.859)	99.90 (a_1') (0.000)	96.51 (e') (0.385)
126.63 (a_2'') (0.003)	139.21 (a_2'') (0.158)	135.13 (a_2'') (0.098)	136.66 (a_1') (0.000)	106.16 (a_2'') (0.931)	101.28 (e'') (0.000)	100.25 (e') (0.628)	97.16 (e'') (0.000)
140.52 (e') (0.023)	148.2 (e') (0.166)	140.24 (e'') (0.000)	136.86 (e'') (0.000)	113.87 (e') (0.000)	103.63 (a_2'') (0.349)	100.94 (a_2'') (0.064)	98.14 (a_2'') (0.027)

158.56 (e') (0.261)	150.78 (e'') (0.000)	141.92 (e') (0.008)	138.23 (a_1'') (0.000)	113.95 (e'') (0.000)	105.77 (a_2') (0.000)	102.07 (a_1'') (0.000)	100.34 (a_2') (0.000)
161.03 (a_2') (0.000)	153.11 (a_2') (0.000)	143.61 (a_2') (0.000)	138.51 (a_2') (0.000)	114.3 (a_2') (0.000)	106.78 (e') (0.018)	102.28 (a_2') (0.000)	101.95 (a_1') (0.000)
163.03 (e'') (0.000)	154.18 (e') (0.966)	145.58 (a_1'') (0.000)	139.18 (e') (0.174)	115.73 (e') (2.651)	108.97 (a_1'') (0.000)	103.84 (e') (0.110)	103.23 (e') (0.229)
166.14 (a_1') (0.000)	158.25 (a_1'') (0.000)	147.7 (e') (0.901)	146.67 (e') (0.827)	119.14 (a_1'') (0.000)	114.49 (e') (1.716)	112.43 (e') (0.857)	111.53 (e') (0.479)
166.8 (e'') (0.000)	163.57 (a_1') (0.000)	161.61 (a_1') (0.000)	160.21 (a_1') (0.000)	120.31 (a_1') (0.000)	118.25 (a_1') (0.000)	118.00 (a_1') (0.000)	117.13 (a_1') (0.000)
168.38 (a_1'') (0.000)	167.76 (e'') (0.000)	167.52 (e'') (0.000)	167.9 (e'') (0.000)	120.56 (e'') (0.000)	121.13 (e'') (0.000)	122.15 (e'') (0.000)	122.19 (e'') (0.000)
173.69 (e') (9.197)	184.64 (e') (1.863)	190.6 (e') (0.010)	189.75 (e') (1.744)	140.33 (e') (1.899)	157.59 (e') (0.051)	158.53 (e') (1.426)	153.23 (e') (3.690)
174.3 (a_2'') (1.051)	188.43 (a_2'') (188.43)	199.68 (a_2'') (0.410)	200.96 (a_2'') (2.987)	141.56 (a_2'') (0.329)	169.81 (a_2'') (0.050)	175.13 (a_2'') (1.033)	170.00 (a_2'') (3.724)

Table S12. Calculated Vibrational Frequencies (in cm^{-1}) as obtained by using PBE/DEF Method for $An@Sb_{12}^{6-}$ and $An@Bi_{12}^{6-}$ Clusters (Intensities in km mol^{-1} and Symmetry are Provided in Parenthesis)

$Th@Sb_{12}^{2-}$	$Pa@Sb_{12}^{-}$	$U@Sb_{12}$	$Np@Sb_{12}^{+}$	$Th@Bi_{12}^{2-}$	$Pa@Bi_{12}^{-}$	$U@Bi_{12}$	$Np@Bi_{12}^{+}$
20.11 (a_2'') (0.185)	33.76 (a_2'') (0.072)	44.13 (e'') (0.000)	36.46 (e'') (0.000)	18.07 (a_2'') (0.294)	33.83 (e'') (0.000)	34.18 (e'') (0.000)	29.29 (e'') (0.000)
34.77 (e'') (0.000)	43.6 (e'') (0.000)	44.42 (a_2'') (0.013)	47.39 (a_2'') (0.000)	26.49 (e'') (0.000)	36.38 (a_2'') (0.136)	37.78 (a_1'') (0.000)	35.70 (a_2') (0.000)
46.27 (e') (0.117)	54.07 (a_1'') (0.000)	54.39 (a_1'') (0.000)	50.75 (e') (0.021)	34.68 (e') (0.027)	38.53 (a_1'') (0.000)	39.24 (a_2') (0.000)	35.96 (e') (0.019)
49.09 (a_1'') (0.000)	54.98 (e') (0.028)	55.47 (e') (0.015)	52.77 (a_1'') (0.000)	36.13 (a_1'') (0.000)	40.47 (e') (0.009)	39.67 (e') (0.006)	36.19 (a_1'') (0.000)
55.46 (a_1') (0.000)	61.56 (a_1') (0.000)	62.09 (a_2') (0.000)	55.87 (a_2') (0.000)	36.17 (a_1') (0.000)	43.05 (a_2') (0.000)	45.13 (a_2'') (0.051)	47.43 (e') (0.003)
72.75 (e') (0.409)	68.29 (a_2') (0.000)	72.99 (a_1') (0.000)	70.41 (e') (0.082)	49.26 (a_2') (0.000)	48.69 (a_1') (0.000)	52.47 (e') (0.032)	47.74 (a_2'') (0.014)
76.33 (a_2') (0.000)	77.17 (e') (0.301)	75.92 (e') (0.178)	76.84 (a_1') (0.000)	51.11 (e') (0.169)	54.0 (e') (0.082)	55.38 (a_1') (0.000)	57.06 (a_1') (0.000)
90.77 (e') (1.001)	99.35 (e') (0.435)	100.89 (e'') (0.000)	98.06 (e') (0.215)	67.9 (e') (0.437)	71.46 (e'') (0.000)	69.46 (e'') (0.000)	66.73 (e'') (0.000)
92.13 (e'') (0.000)	101.07 (e'') (0.000)	101.03 (e') (0.176)	98.12 (e'') (0.000)	68.01 (e'') (0.000)	72.24 (e') (0.028)	73.38 (e') (0.000)	71.94 (e') (0.004)
105.56 (a_1') (0.000)	111.27 (a_1') (0.000)	112.12 (a_1') (0.000)	111.12 (a_1') (0.000)	78.68 (a_1') (0.000)	83.41 (a_1') (0.000)	85.27 (a_1') (0.000)	85.47 (a_1') (0.000)
113.59 (e') (0.081)	128.76 (e') (0.131)	126.04 (e') (0.125)	117.32 (e') (0.033)	92.38 (e') (0.523)	101.08 (e') (0.536)	97.67 (e') (0.384)	89.97 (e') (0.207)
115.55 (a_1') (0.000)	133.27 (a_2'') (0.005)	131.04 (a_2'') (0.000)	128.67 (a_2'') (0.009)	92.92 (a_1') (0.000)	101.09 (e'') (0.000)	100.56 (e'') (0.000)	99.94 (a_2'') (0.016)
127.38 (a_2'') (0.012)	133.38 (a_1') (0.000)	138.89 (e'') (0.000)	138.51 (e'') (0.000)	103.74 (a_2'') (0.241)	102.33 (a_1') (0.000)	101.74 (a_2'') (0.006)	100.37 (a_1'') (0.000)
138.52 (e') (0.153)	143.86 (e'') (0.000)	141.66 (a_1') (0.000)	138.85 (a_2') (0.000)	107.9 (e'') (0.000)	102.7 (a_2'') (0.024)	104.17 (a_2') (0.000)	100.59 (e'') (0.000)
158.03 (e'') (0.000)	144.8 (e') (0.003)	143.24 (a_2') (0.000)	139.7 (e') (0.244)	111.46 (e') (0.126)	106.62 (a_2') (0.000)	104.37 (a_1'') (0.000)	102.13 (a_2') (0.000)

158.83 (e') (0.439)	149.8 (a_2') (0.000)	143.73 (e') (0.111)	140.14 (a_1'') (0.000)	112.01 (a_2') (0.000)	107.81 (e') (0.004)	105.32 (a_1') (0.000)	103.79 (e') (0.088)
159.81 (a_2') (0.000)	152.15 (e') (0.402)	145.12 (a_1'') (0.000)	144.26 (a_1') (0.000)	114.42 (e') (0.819)	108.66 (a_1'') (0.000)	106.1 (e') (0.082)	105.96 (a_1') (0.000)
164.94 (a_1'') (0.000)	153.05 (a_1'') (0.000)	150.18 (e') (0.361)	151.2 (e') (0.652)	115.2 (a_1'') (0.000)	114.58 (e') (0.540)	114.25 (e') (0.409)	113.75 (e') (0.543)
167.72 (a_1') (0.000)	167.57 (a_1') (0.000)	166.99 (a_1') (0.000)	164.57 (a_1') (0.000)	121.52 (a_1') (0.000)	122.71 (a_1') (0.000)	122.46 (a_1') (0.000)	120.63 (a_1') (0.000)
169.44 (e'') (0.000)	170.77 (e'') (0.000)	171.96 (e'') (0.000)	171.55 (e'') (0.000)	122.89 (e'') (0.000)	125.32 (e'') (0.000)	126.53 (e'') (0.000)	125.71 (e'') (0.000)
176.92 (e') (4.070)	184.27 (e') (0.425)	184.29 (e') (0.182)	180.62 (e') (1.586)	139.79 (e') (0.684)	147.51 (e') (0.092)	144.24 (e') (1.120)	139.06 (e') (2.607)
177.15 (a_2'') (0.430)	189.37 (a_2'') (0.001)	194.31 (a_2'') (0.952)	191.89 (a_2'') (3.736)	144.86 (a_2'') (0.111)	160.45 (a_2'') (0.154)	161.71 (a_2'') (1.202)	157.51 (a_2'') (3.492)

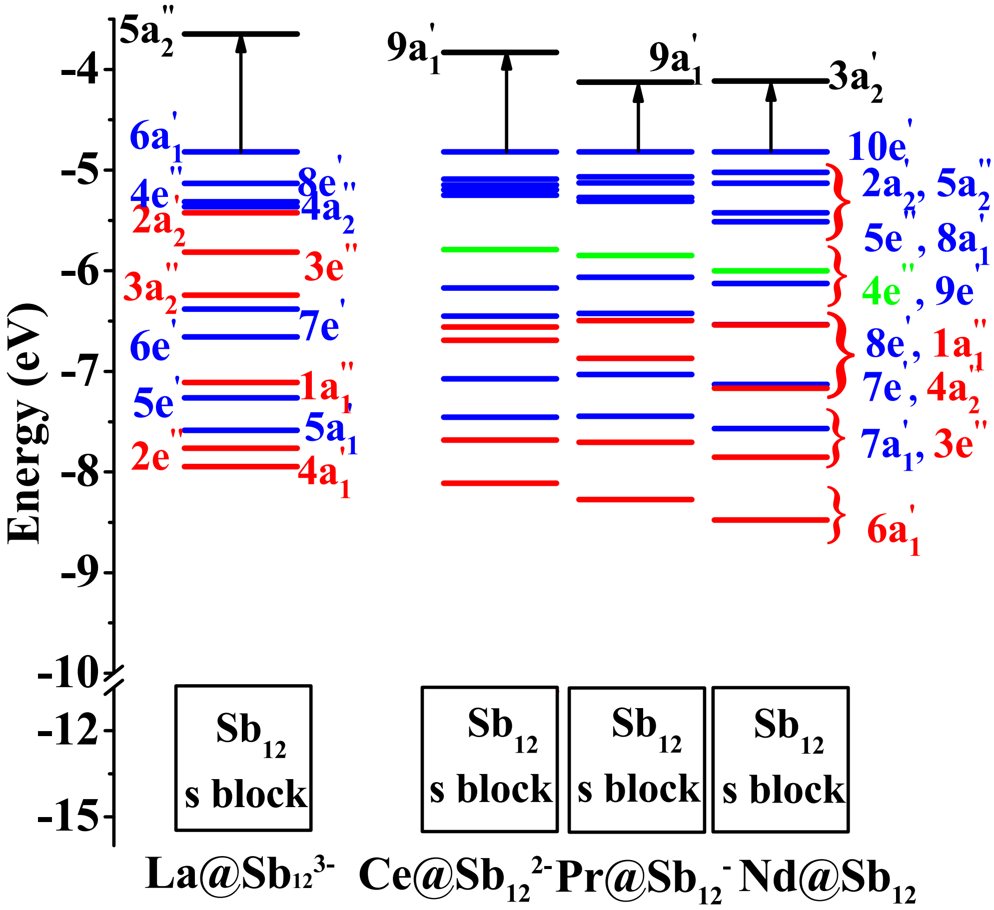

Figure S1. Molecular orbital energy level diagram of $Ln@Sb_{12}^{6-}$ (Ln = La^{3+}, Ce^{4+}, Pr^{5+}, Nd^{6+}) clusters in D_{3h} symmetry as obtained by using PBE/DEF method. (Where blue lines represents mixed MOs having orbital contribution from central metal ion and ring atoms, red lines stands for the MOs corresponding to the pure orbital of ring atoms only and green lines stands for small mixed MOs having small contribution of central ion orbitals. Here, the s block refers to the valence s−orbitals of Sb atoms)

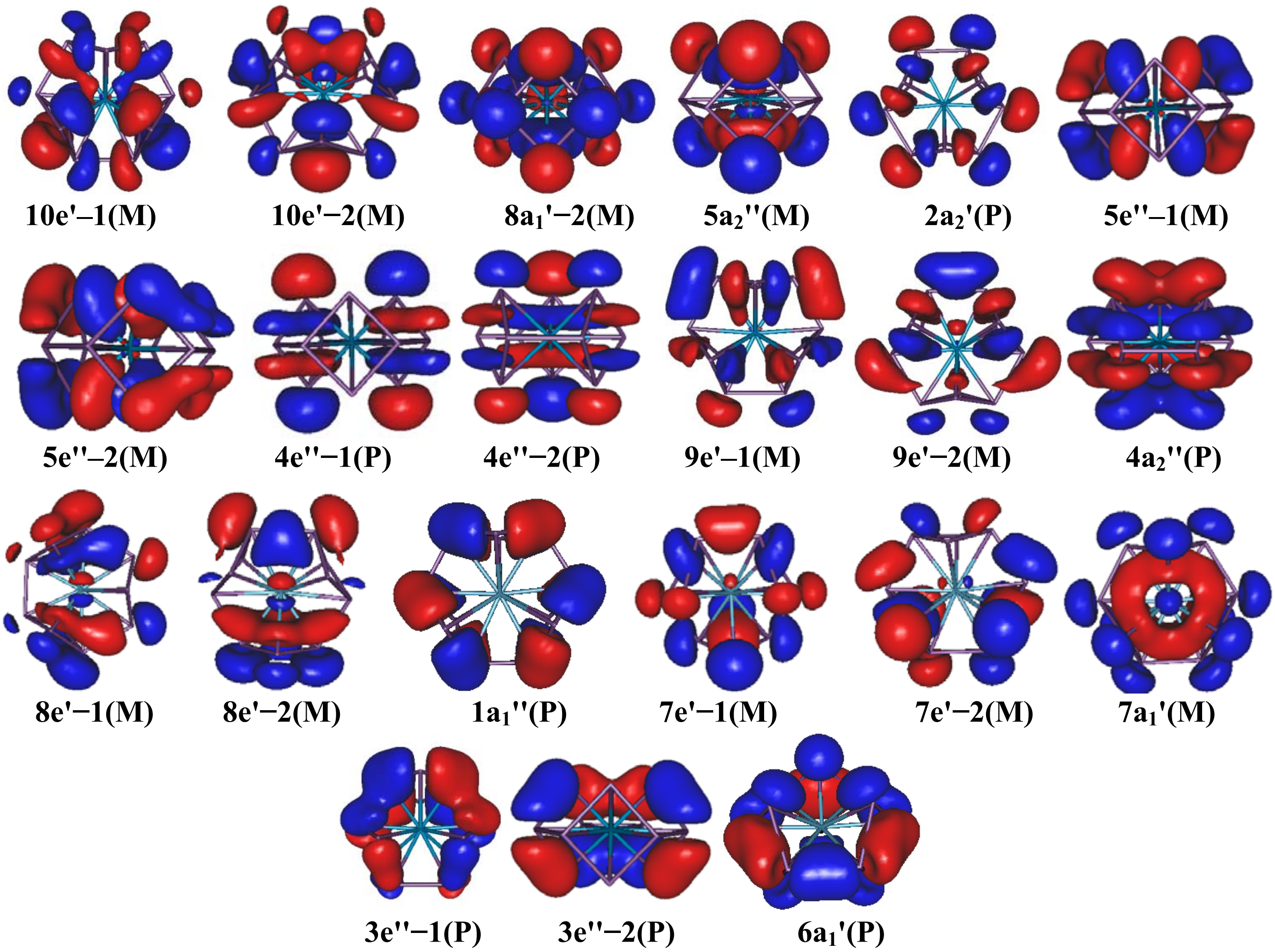

As, it can be seen from the above MOs pictures, that no f orbitals of Th are involved in the bonding with ring atoms. Therefore, in the present system, intra ring bonds are not elongated. Therefore, in $Th@Sb_{12}^{2-}$ system, all R_{intra} bonds are shorter than the R_{inter} bonds.

Figure S2. Molecular orbital pictures of $Th@Sb_{12}^{2-}$ cluster in D_{3h} symmetry as obtained by using PBE/DEF method. (Where M stands for mixed MOs having orbital contribution from central metal atom and ring atoms, P stands for MOs corresponds to pure orbital of ring atoms alone)

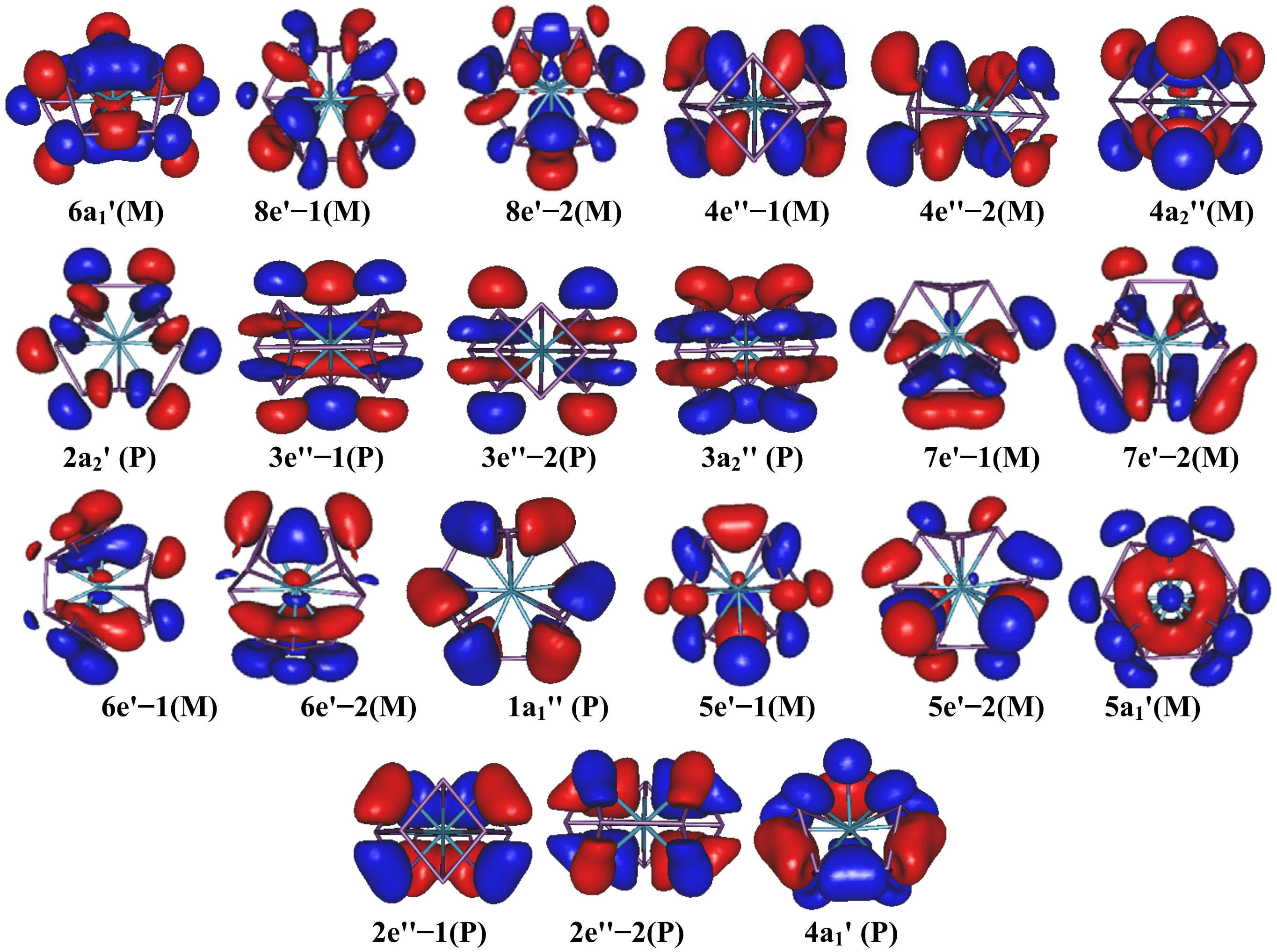

As, it can be seen from the above MOs pictures, that no f orbitals of La are involved in the bonding with ring atoms. Therefore, in the present system, intra ring bonds are not elongated. Therefore, in $La@Sb_{12}^{3-}$ system, all R_{intra} bonds are shorter than the R_{inter} bonds.

Figure S3. Molecular orbital pictures of $La@Sb_{12}^{3-}$ cluster in D_{3h} symmetry as obtained by using PBE/DEF method. (Where M stands for mixed MOs having orbital contribution from central metal ion and ring atoms, P stands for MOs corresponds to pure orbital of ring atoms only)

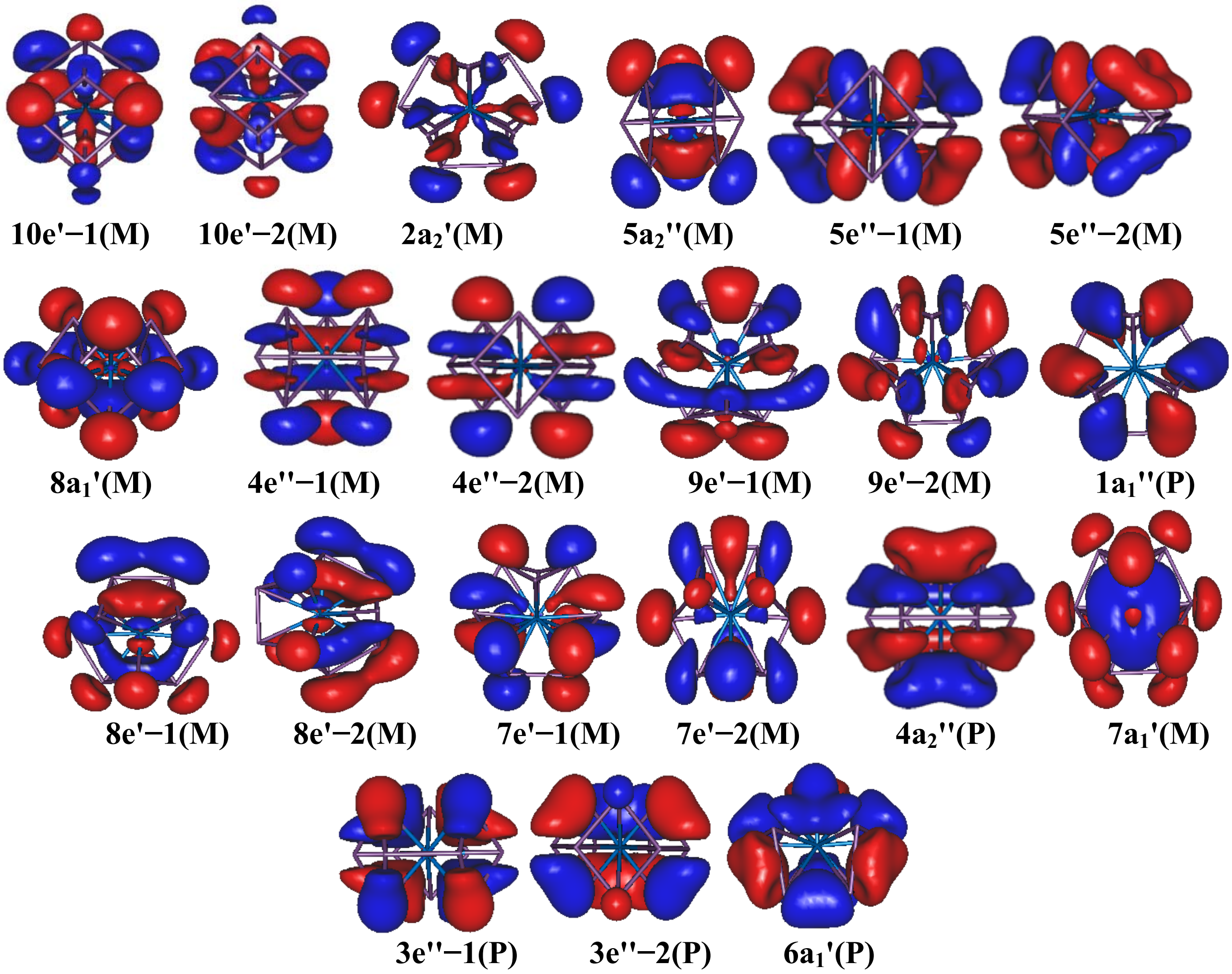

As, it can be seen from the above MOs pictures, that the f orbitals of U are involved in the bonding with ring atoms in 10e' and $2a_2$' MOs. Therefore, in the present system, intra ring bonds are elongated and became longer than the R_{inter} bonds.

Figure S4. Molecular orbital pictures of U@Sb_{12} cluster in D_{3h} symmetry as obtained by using PBE/DEF method. (Where M stands for mixed MOs having orbital contribution from central metal atom and ring atoms, P stands for MOs corresponds to pure orbital of ring atoms alone)

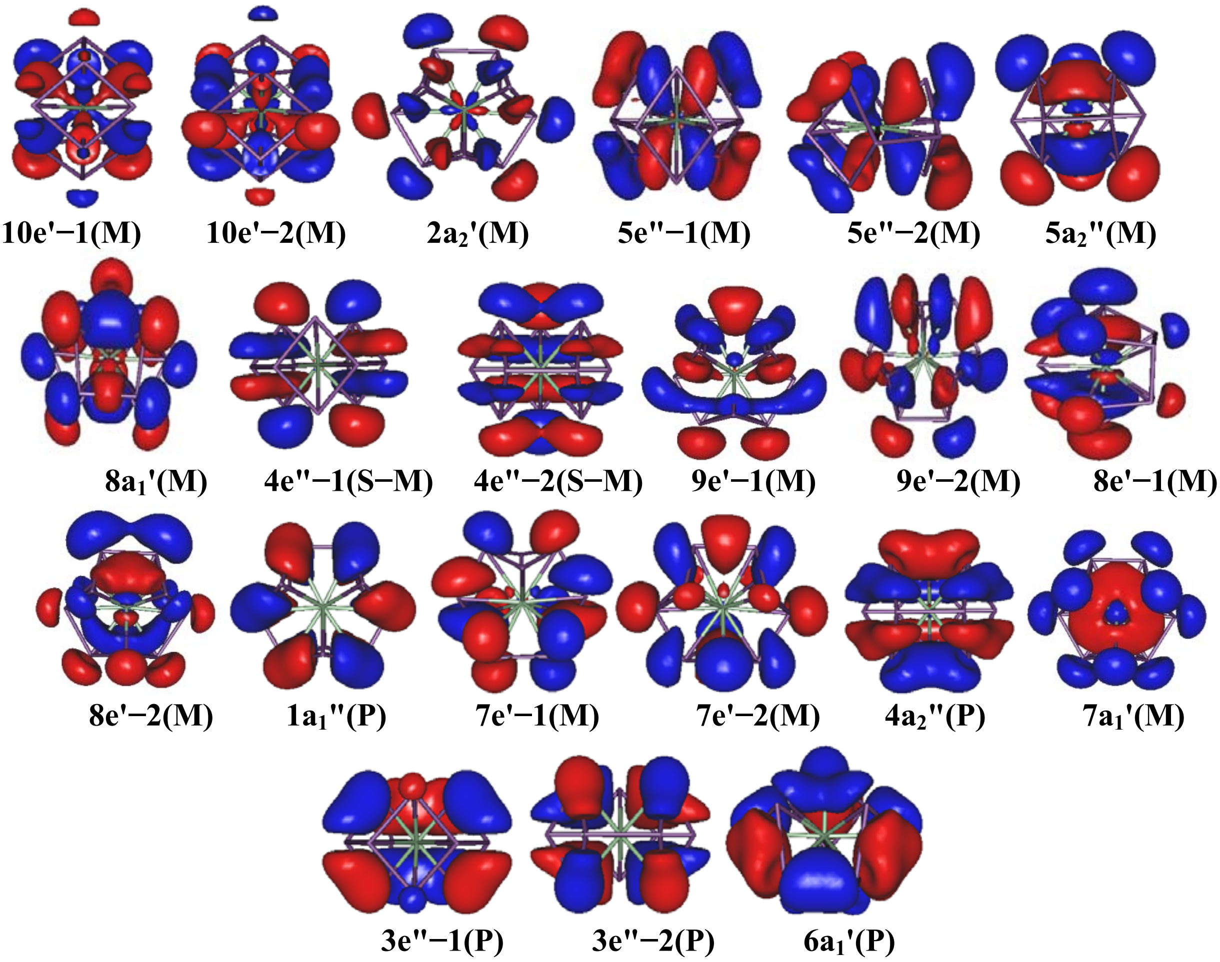

As, it can be seen from the above MOs pictures, that the f orbitals of Nd are involved in the bonding with ring atoms in 10e' and 2a$_2$' MOs. Therefore, in the present system, intra ring bonds are elongated and became longer than the R_{inter} bonds.

Figure S5. Molecular orbital pictures of Nd@Sb_{12} cluster in D_{3h} symmetry as obtained by using PBE/DEF method. (Where M stands for mixed MOs having orbital contribution from central metal ion and ring atoms, P stands for MOs corresponds to pure orbital of ring atoms only and S−M stands for those MOs which are formed by the overlapping of atomic orbital of ring atoms and have very small overlapping with the atomic orbital of central atom)

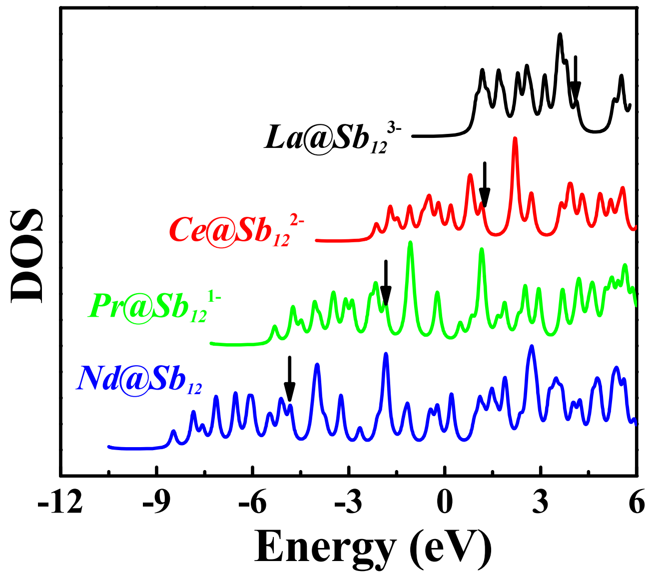

Figure S6. Density of states plots of $Ln@Sb_{12}^{6-}$ (Ln = La^{3+}, Ce^{4+}, Pr^{5+}, Nd^{6+}) clusters in D_{3h} symmetry as obtained by using PBE/DEF method. (Arrows are showing peak corresponding to HOMO).

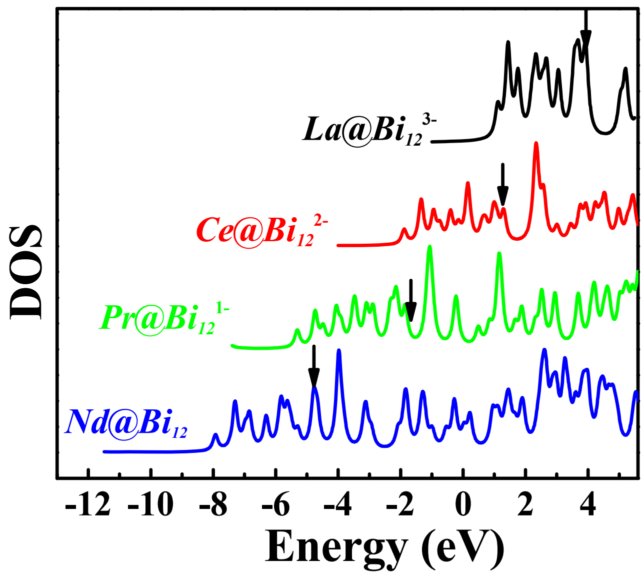

(a)

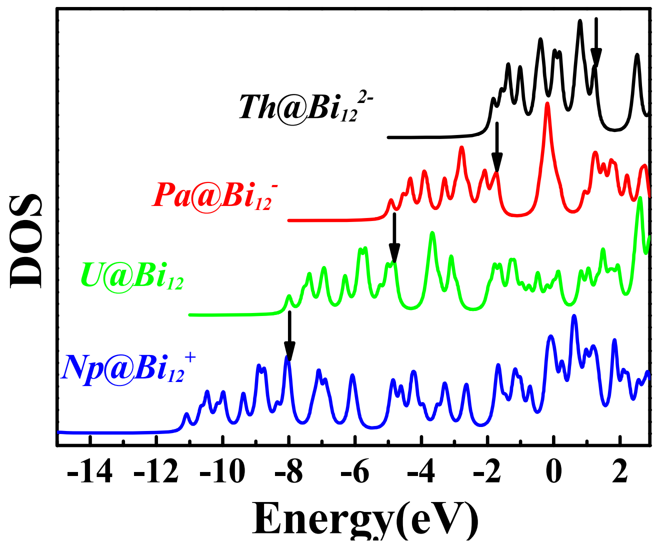

(b)

Figure S7. Density of states plots of (a) $Ln@Bi_{12}^{6-}$ (Ln = La^{3+}, Ce^{4+}, Pr^{5+}, Nd^{6+}) clusters and (b) $An@Bi_{12}^{6-}$(An = Th^{4+}, Pa^{5+}, U^{6+}, Np^{7+}) clustersin D_{3h} symmetry as obtained by using PBE/DEF method. (Arrows are showing peak corresponding to HOMO).

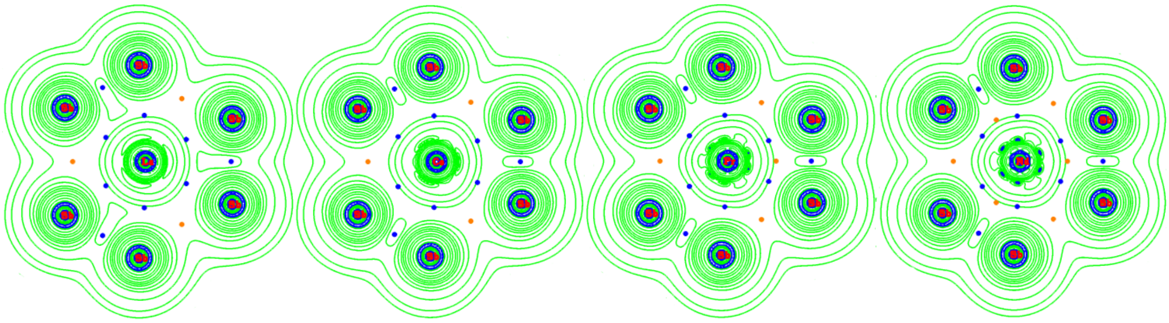

(a1)

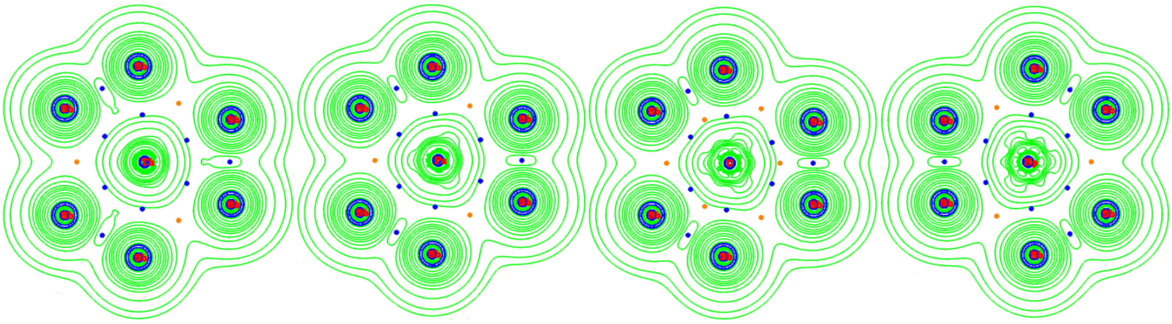

(a2)

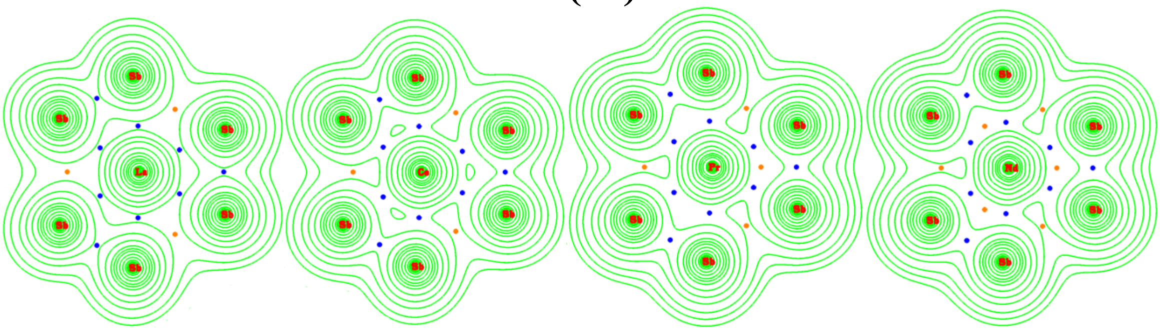

(b1)

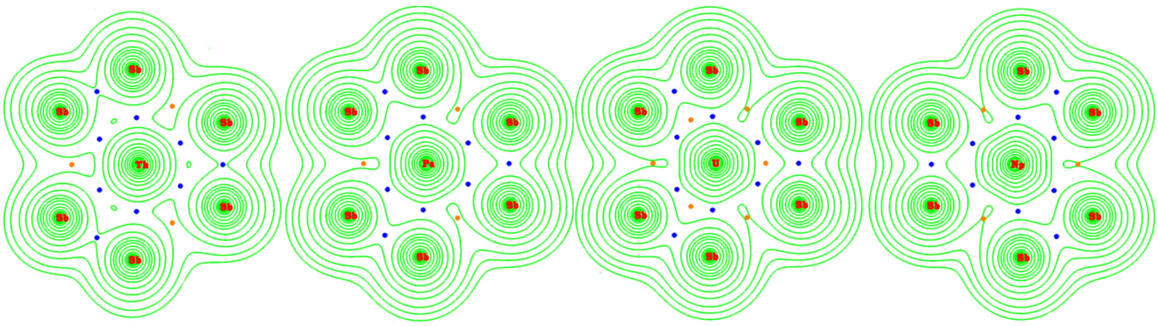

(b2)

Figure S8. Laplacian of electron density plots (a1 & a2) and Electron density plots (b1 & b2) of $Ln@Sb_{12}^{6-}$ and $An@Sb_{12}^{6-}$ clusters, respectively, in D_{3h} symmetry as obtained by using PBE/DEF method employed with EDF. (Blue dots are Bond critical point (BCP) and orange dots are ring critical point (RCP))

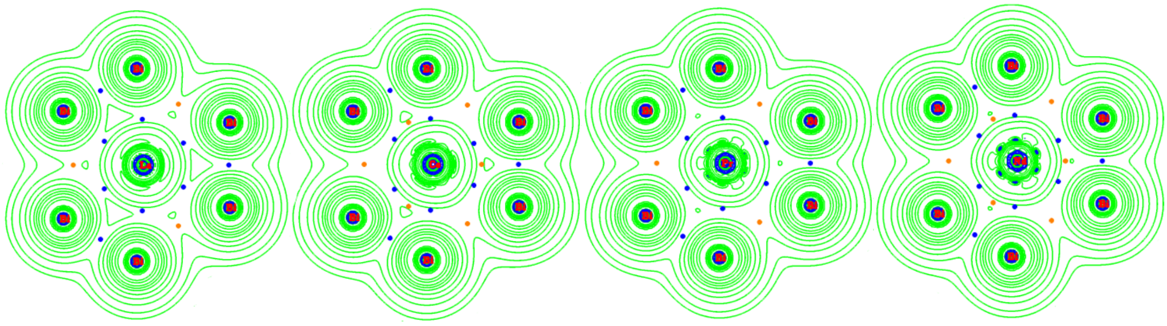

(a1)

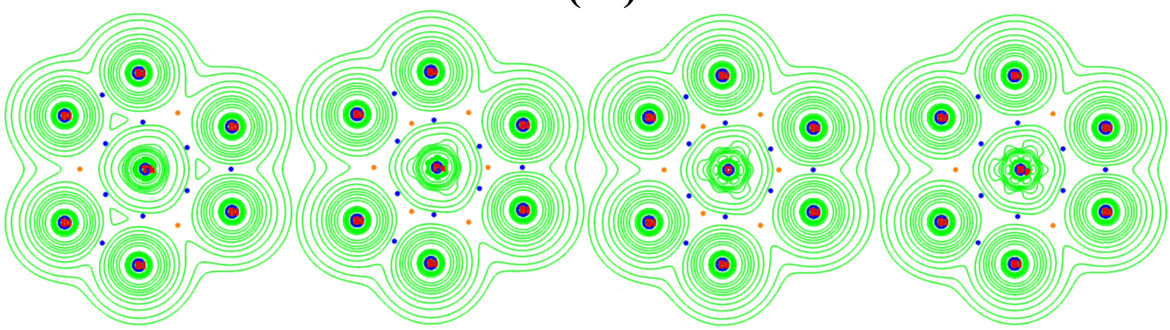

(a2)

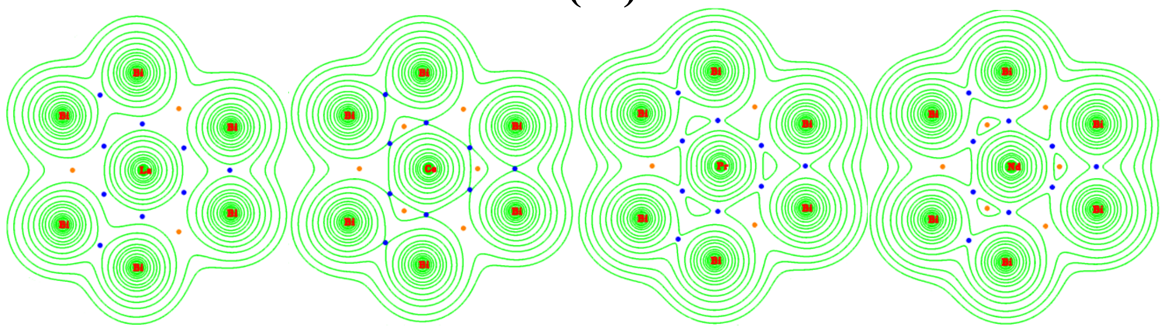

(b1)

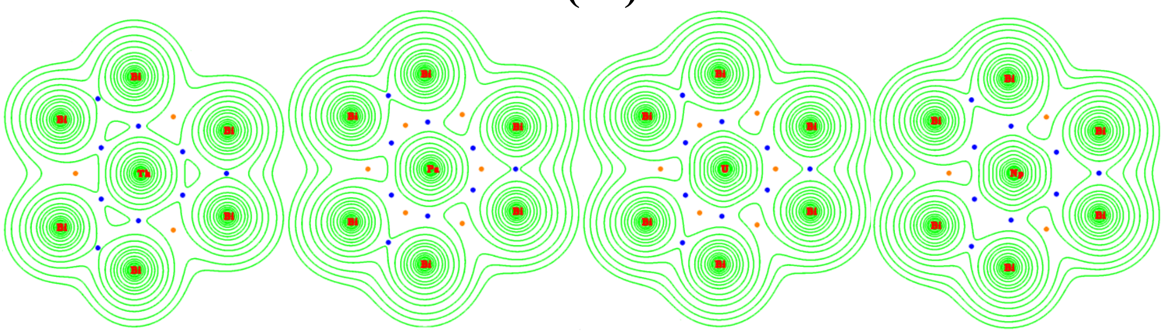

(b2)

Figure S9. Laplacian of electron density plots (a1 & a2) and Electron density plots (b1 & b2) of Ln@Bi$_{12}$$^{6-}$ and An@Bi$_{12}$$^{6-}$ clusters, respectively, in D$_{3h}$ symmetry as obtained by using PBE/DEF methodemployed with EDF. (Blue dots are bond BCP and orange dots are ring critical point (RCP))

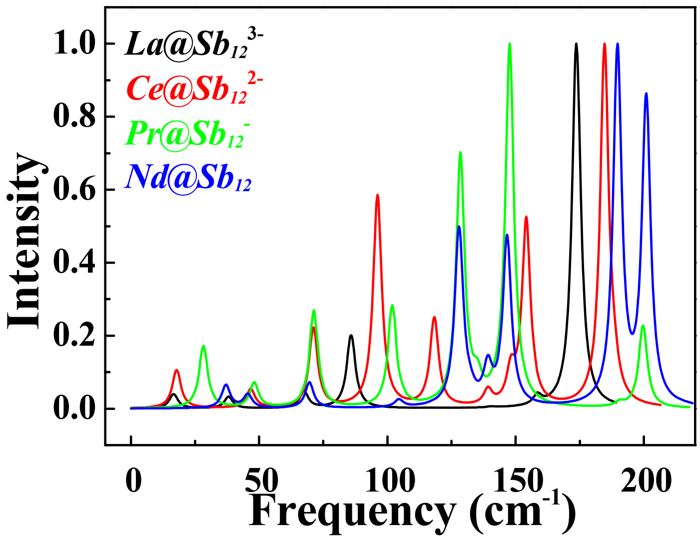

(a)

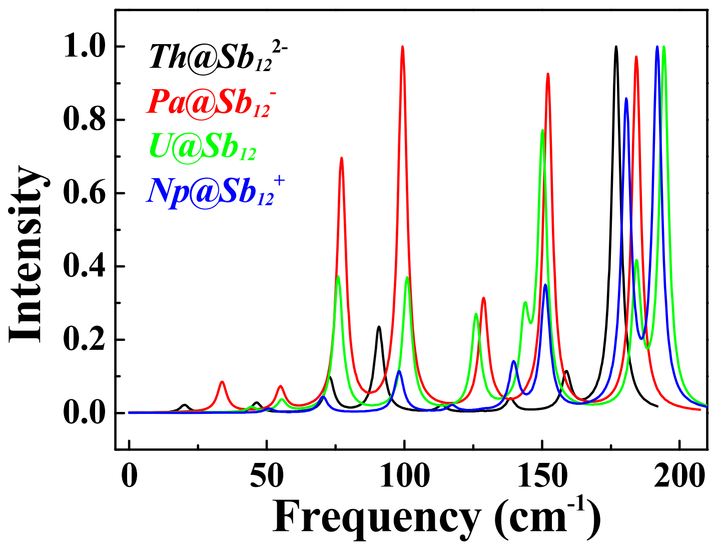

(b)

Figure S10. Harmonic frequency plots of (a) $Ln@Sb_{12}^{6-}$ and (b) $An@Sb_{12}^{6-}$ clusters, respectively, in D_{3h} symmetry as obtained by using PBE/DEF method.

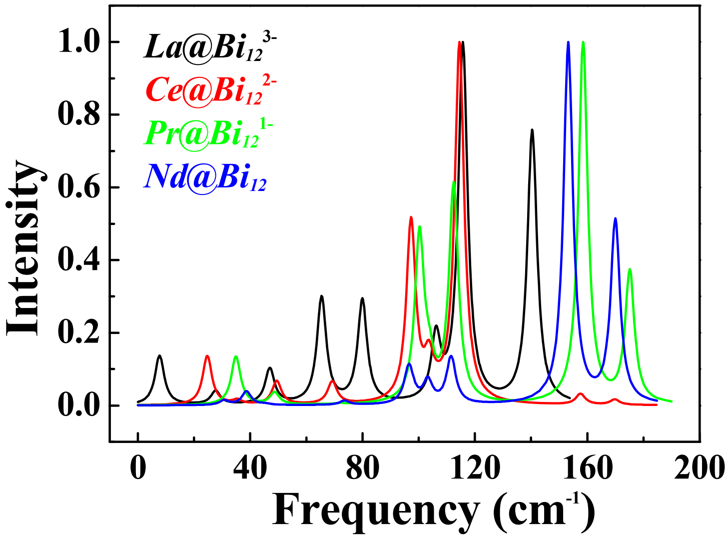

(a)

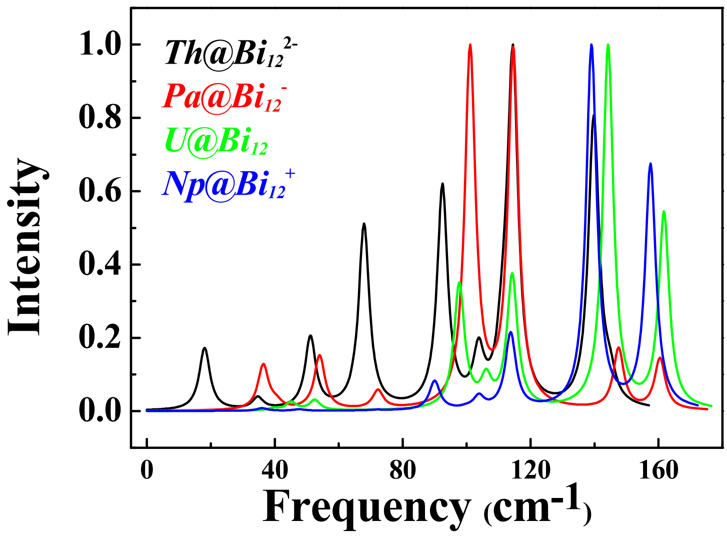

(b)

Figure S11. Harmonic frequency plots of (a) Ln@Bi_{12}^{6-} and (b) An@Bi_{12}^{6-} clusters, respectively, in D_{3h} symmetry as obtained by using PBE/DEF method.

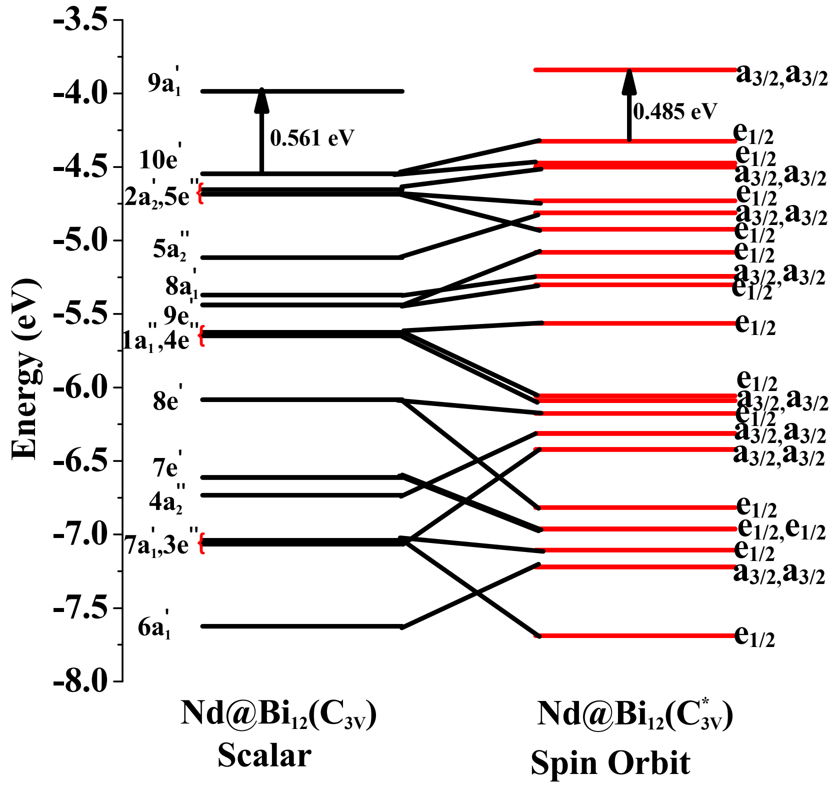

Figure S12. Scalar relativistic (left panel) and spin orbit splitting (right panel) diagram of the valence molecular orbital energy levels of Nd@Bi_{12} system.

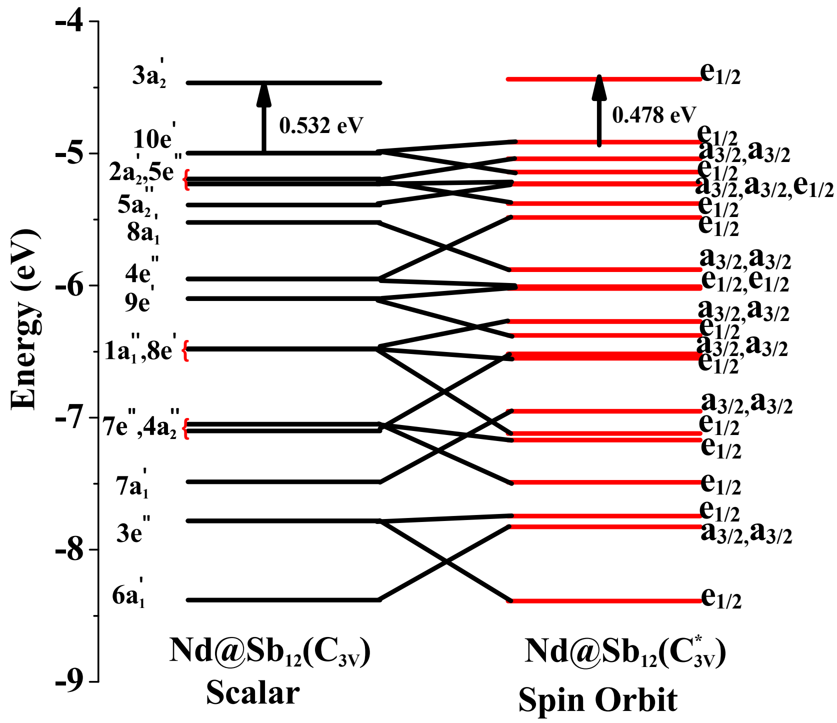

Figure S13. Scalar relativistic (left panel) and spin orbit splitting (right panel) diagram of the valence molecular orbital energy levels of Nd@Sb_{12} system.

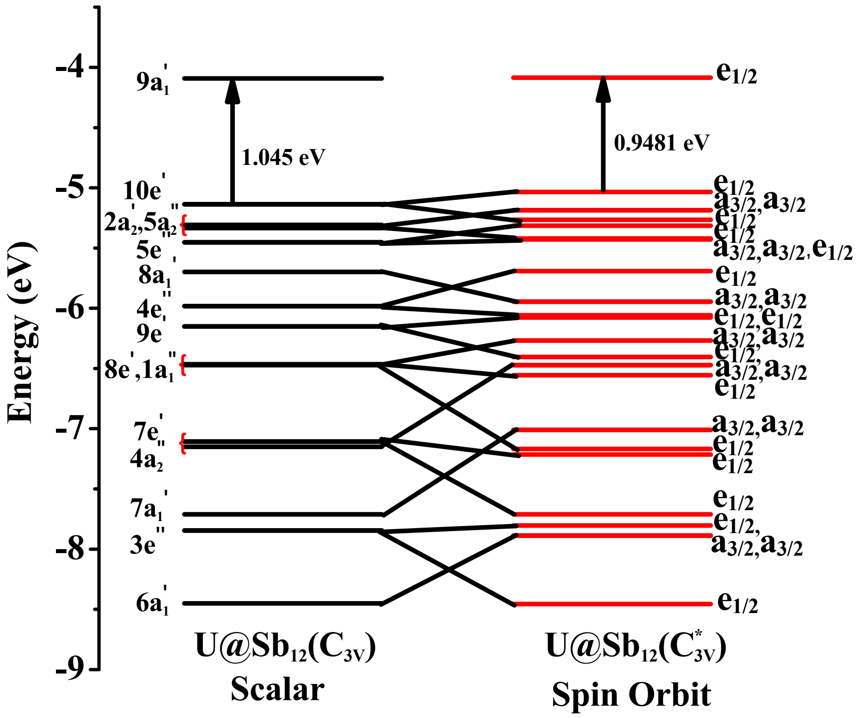

Figure S14. Scalar relativistic (left panel) and spin orbit splitting (right panel) diagram of the valence molecular orbital energy levels of U@Sb$_{12}$ system.